FUNCTIONAL CONSEQUENCES OF ULTRASTRUCTURAL GEOMETRY IN "BACKWARDS" FLUID-TRANSPORTING EPITHELIA

JARED M. DIAMOND and WILLIAM H. BOSSERT

From the Department of Physiology, University of California at Los Angeles School of Medicine, Los Angeles, California 90024, and the Biological Laboratories and Division of Applied Mathematics, Harvard University, Cambridge, Massachusetts 02138

ABSTRACT

Many fluid-transporting epithelia possess dead-end, long, and narrow channels opening in the direction to which fluid is being transported (basal infoldings, lateral intercellular spaces, etc.). These channels have been thought to possess geometrical significance as standing-gradient flow systems, in which active solute transport into the channel makes the channel contents hypertonic and permits water-to-solute coupling. However, some secretory epithelia (choroid plexus, Malpighian tubule, rectal gland, etc.) have "backwards" channels opening in the direction from which fluid is being transported. It is shown that these backwards channels can function as standing-gradient flow systems in which solute transport *out* of the channel makes the channel contents hypotonic and results in coupled water flow *into* the channel mouth. The dependence of the transported osmolarity (isotonic or hypertonic) on channel radius, length, and other parameters is calculated for backwards channels for values of these parameters in the physiological range. In addition to backwards channels' being hypotonic rather than hypertonic, they are predicted to differ from "forwards" channels in that some restrictions are imposed by the problem of solute exhaustion, and in the presence of a sweeping-in effect on other solutes which limits the solutes that may be transported.

Most epithelial cells carrying out coupled transport of solutes and water are found to be constructed on a common geometrical plan: they possess long and narrow dead-end channels oriented parallel to the direction of fluid transport, open at the end towards which fluid is being transported but closed at the end from which fluid is being absorbed. Examples of such structures are lateral intercellular spaces (gallbladder, small intestine, rat proximal tubule), basal infoldings (distal tubule, salivary gland striated duct), bile canaliculi (liver), intracellular canaliculi of the parietal cells (stomach), and perhaps microvilli (intestine, proximal tubule, gallbladder). Lateral intercellular spaces have been shown to be the route of fluid transport in rabbit gallbladder (3, 4, 6, 13), and there is suggestive evidence that these channels may also serve as the route in some other organs. They will be referred to in this paper as "forwards" channels.

In some secretory epithelia one finds long and narrow channels oriented backwards, i.e. with the open end facing the side of the epithelium from which fluid is being taken up. For instance, the ependymal cells of the choroid plexus (10), the cells of elasmobranch rectal gland (1), and the epithelial cells of insect Malpighian tubule (14; Berridge, M. Personal communication) resemble

absorptive cells morphologically since they possess an extensively infolded basal membrane (facing the bloodstream) and a microvillous brush border at the luminal surface. Nevertheless, the direction of transport in both cases is secretory, i.e., from blood to lumen. If fluid transport in these organs involves basal infoldings and microvilli (an unproven, though plausible, assumption), the flow directions would have to be opposite to those in the long and narrow channels of absorptive epithelia: solute and water would *enter* the open mouth of a basal infolding from the blood and would pass from the infolding *into* the cell and from the microvilli *into* the lumen of the brain ventricle or the Malpighian tubule. The basal infoldings found in the nasal salt gland of birds (7), the lateral intercellular spaces of the salt gland of marine turtles (5, 12), and the intracellular tubules of chloride cells of euryhaline fish (8, 9) are also oriented backwards. This morphological similarity between absorptive and secretory cells poses a challenge to any theory linking epithelial ultrastructure with function. We shall be concerned here only with the functional interpretation of these morphological features, since the existence of these features is adequately documented experimentally.

It has been argued that the long and narrow forwards channels of epithelia constitute standing-gradient flow systems and that their morphology has a geometrical significance in permitting coupling of water transport to active solute transport (2, 4, 13). Active solute transport into the channel lumen would maintain the channel contents hypertonic, with the osmolarity decreasing progressively from a maximum value at the closed end to isotonicity at the open end. Water would flow progressively into the channel osmotically across its walls owing to this standing osmotic gradient, and a fluid of constant osmolarity (isotonic or hypertonic, depending upon the parammeters of the system) would continually emerge from the open mouth of this flow system (Fig. 1, top). Insertion of measured values for solute transport rates and diffusion coefficients, water permeabilities, and channel lengths and radii into the differential equation describing the system showed that this reconstruction could account for many distinctive properties of transporting epithelia. The development of standing osmotic gradients in epithelial channels seems inevitable if their

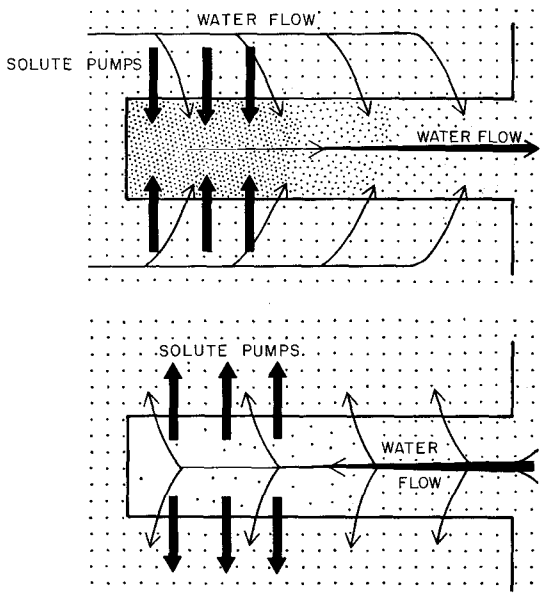

FIGURE 1 Comparison of "forwards" and "backwards" operation of a standing-gradient flow system, which consists of a long narrow channel closed at one end (e.g., a basal infolding, lateral intercellular space, etc.). The density of dots indicates the solute concentration. Forwards operation (top): solute is actively transported into the channel across its walls, making the channel fluid hypertonic. As solute diffuses down its concentration gradient towards the open mouth, more and more water enters the channel across its walls due to the osmotic gradient. In the steady state a standing osmotic gradient will be maintained in the channel by active solute transport, with the osmolarity decreasing progressively from the closed end to the open end; and a fluid of fixed osmolarity (isotonic or hypertonic, depending upon the values of such parameters as radius, length, and water permeability) will constantly emerge from the mouth. Backwards operation (bottom): solute is actively transported out of the channel across its walls, making the channel fluid hypotonic. As solute diffuses down its concentration gradient towards the closed end, more and more water leaves the channel across its walls owing to the osmotic gradient. In the steady state a standing osmotic gradient will be maintained in the channel by active solute transport, with the osmolarity decreasing progressively from the open end to the closed end; and a fluid of fixed osmolarity (isotonic or hypertonic, depending upon the parameters of the system) will constantly enter the channel mouth and be secreted across its walls. Solute pumps are depicted only at the bottom of the channels for illustrative purposes but may have different distributions along the channel.

fluid contents are effectively unstirred, as is almost surely the case.

The purpose of the present paper is to show that backwards channels are readily explained by the standing-gradient hypothesis and hence may also possess geometrical significance. If solute is actively taken up *out of* the channel lumen and transported across the channel wall, the channel lumen will become hypotonic rather than hypertonic (Fig. 1, bottom). A standing osmotic gradient will be maintained in which channel osmolarity progressively *decreases* from isotonicity at the open end to a minimum value at the closed end. Water will leave the channel across its walls by osmosis, at increasing rates along its length, because the lumen is increasingly hypotonic. In the steady state a fluid of fixed osmolarity (isotonic or hypertonic, depending upon the parameters of the system) will continually pass into the mouth of the channel and be taken up across the channel walls. This paper explores the predicted functional differences between backwards and forwards channels in the light of sample calculations for a backwards standing-gradient flow system, using values of model parameters in the physiological range. The mathematical treatment follows that of our paper on forwards channels (2) which should be consulted for further details and discussion of assumptions and idealizations.

MATERIALS AND METHODS

Let us consider a dead-end, right-circular-cylindrical channel whose walls are a semipermeable membrane, oriented along the x axis, with the closed end at $x = 0$ and the open end at $x = L$. The length of the channel is therefore L; the radius is represented by r; the osmotic water permeability of the channel walls (volume of fluid crossing 1 cm^2 in 1 sec in response to an osmotic gradient of 1 osmol/liter) by P; the osmolarity of the fluid outside the channel (e.g. the osmolarity of the intracellular fluid, assumed identical with that of the bathing solutions) by C_o; the diffusion coefficient of the actively transported solute by D; and the rate of active solute transport across the walls of the channel into its lumen at any height x (milliosmols of solute transported in 1 sec across 1 cm^2 of channel wall area) as $N(x)$. The dependent variables are $C(x)$, the osmolarity of the fluid in the channel at a height x; and $v(x)$, the linear velocity of fluid flow in the channel at height x, taken as positive in the direction $x = 0$ to $x = L$. The problem is to find the osmolarity of the fluid continually passing in the steady state into the open mouth of the channel, given by the expression $2\pi r \frac{\int_{x=0}^{x=L} N(x)\,dx}{\pi r^2 v(L)}$ (referred to subsequently as expression 1).

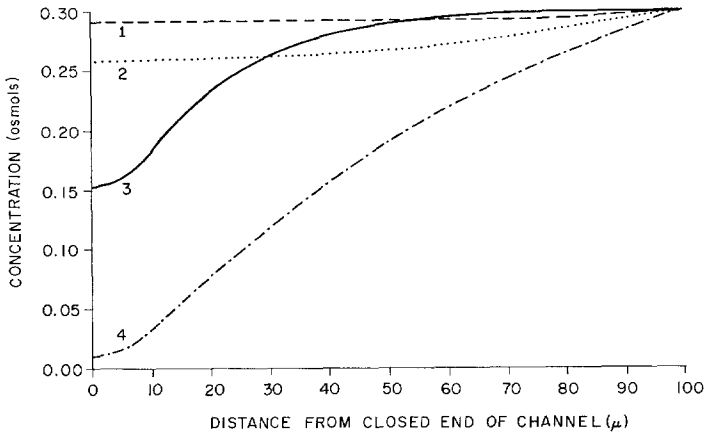

FIGURE 2 Examples of concentration profiles in a standing-gradient flow system functioning backwards. The solute concentration in the channel in the steady state (ordinate) is plotted against x, the linear distance from the closed end of the channel (abscissa). L was held fixed at 100 μ, r at 0.05 μ, C_o at 0.3 osmol, and D at 10^{-5} cm^2/sec. P was 4×10^{-5} (curve *1*), 1×10^{-5} (curve *2*), 2×10^{-5} (curve *3*), or 2×10^{-6} (curve *4*) cm/sec, osmol. N was -1.11111×10^{-7} milliosmols/cm^2, sec for $0 < x < 90$ μ, zero for $90 < x < 100$ μ (curve *1*); -1.25×10^{-7} for $0 < x < 80$ μ, zero for $80 < x < 100$ μ (curve *2*); or -2×10^{-6} (curve *3*) or -1.15×10^{-6} (curve *4*) for $0 < x < 10$ μ, zero for $x > 10$ μ. The corresponding calculated concentrations of the transported fluid (given by expression 1) were 0.322 (curve *1*), 0.352 (curve *2*), 0.300 (curve *3*), and 0.455 (curve *4*) osmol.

As shown previously (2), the differential equation describing the system is

$$N(x) + \frac{Dr^2}{4P}\frac{d^3v}{dx^3} - \frac{r^2v}{4P}\frac{d^2v}{dx^2} - \frac{C_o r}{2}\frac{dv}{dx} - \frac{r^2}{4P}\left(\frac{dv}{dx}\right)^2 = 0$$

with the boundary conditions $dC/dx = 0 = d^2v/dx^2$ at $x = 0$; $v = 0$ at $x = 0$; and $C(x) = C_o$ at $x = L$. Computations were carried out on the IBM 7094 computer by the same procedures as before, except that the variable $C(x)$ was transformed into $C(x) - C_o$ to permit greater precision of representation of concentrations near C_o, and fourth order instead of second order Runge-Kutta formulae were used.

The ranges of numerical values of r, L, P, $N(x)$, and D are those used and justified previously (reference 2, pages 2068–2069) to cover the experimental ranges of channel radii, lengths, and permeabilities, solute transport rates, and diffusion coefficients observed experimentally in epithelia. The only difference is that values of $N(x)$ were taken as negative. This represents solute transport out of, rather than into, the channel.

RESULTS

Concentration and Velocity Profiles

Figs. 2 and 3 give concentration and velocity profiles calculated for four different sets of model parameters. Channel osmolarity is isotonic at the open end and always becomes progressively lower (more hypotonic) towards the closed end (Fig. 2). The extent of the hypotonicity and the form of the profile depend upon values of the model parameters. Channel hypotonicity is more marked (osmolarity lower) for higher values of solute transport rate and channel length, and for lower values of channel water permeability and radius and solute diffusion coefficient. No general correlation exists between the standing osmolarity of the channel fluid, which is always hypotonic or isotonic, and the effective moving osmolarity of the transported fluid (given by the ratio of solute uptake to water uptake across the channel walls, i.e., by expression 1), which is always isotonic or hypertonic. The reason for this lack of correlation is that solute flux into the channel mouth is governed both by the sweeping effect of the water flow and by solute diffusion down its concentration gradient, as has been discussed previously (reference 2, page 2077). The linear flow velocity from open to closed end is maximum at the open end and decreases progressively towards the closed end as more and more fluid passes out across the channel walls (Fig. 3).

One of the two principal differences between

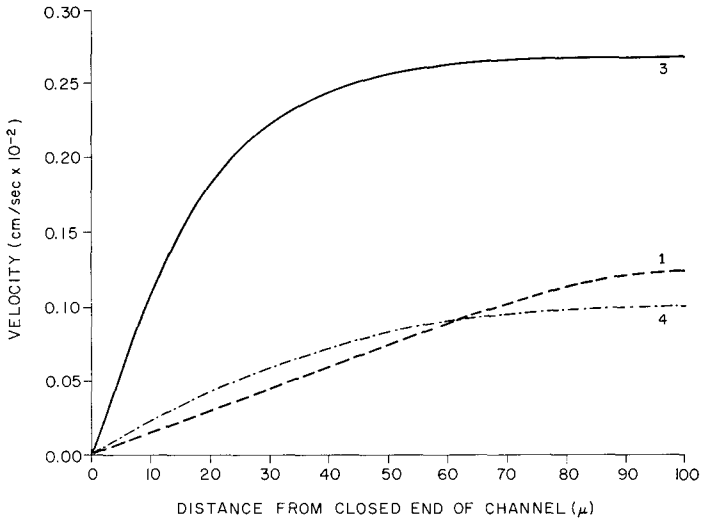

FIGURE 3 Examples of velocity profiles in a backwards standing-gradient flow system, corresponding to the concentration profiles of Fig. 2. The linear velocity of water flow in the channel in the steady state (ordinate) is plotted against x, the linear distance from the closed end of the channel (abscissa). The direction of flow is from the open end to the closed end, so that these velocities are negative by the sign convention we used. Symbols and values as in Fig. 2. Curve *2* is omitted for clarity because it lies between curves *1* and *4*.

forwards and backwards operation of a standing-gradient flow system follows from Fig. 2. In a forwards epithelium, where solute is transported into the channel and the channel becomes hypertonic, there are no restrictions to this hypertonicity except those imposed by the solubility of the transported solute; hence, there are no other restrictions on possible values of model parameters. In a backwards epithelium, where solute is transported out of the channel and the channel becomes hypotonic, it is physically impossible for channel osmolarity and solute concentration to drop below zero at any point. For instance, in curve *4* of Fig. 2 the concentrations near the closed end of the channel (left-hand side of the figure) are close to this zero-concentration limit. In practice, this problem of solute exhaustion imposes a maximum possible value on the transport rate $N(x)$ for a given set of values of the other model parameters, whereas no such limit except that associated with saturated solution concentrations arises in the forwards channel case. (These limits will also be illustrated in connection with Figs. 5 and 6.) More specifically, for any distribution $f(x)$ of the transport mechanism along the channel wall such that $N(x) = kf(x)$, there will be some value of k at which $C(0) = 0$, and higher values of k are physically impossible. This suggests that, all other things being equal, backwards epithelia may have to have more channels or higher water permeabilities or lower transport rates than forwards epithelia.

Transport Site

The solute pumps might be distributed uniformly along the length of the channel, or they might be concentrated in part of the channel. Fig. 4 illustrates the effect upon the transported osmolarity of varying the distance from the closed end of the channel over which solute input takes place, while maintaining the same total rate of input for the whole channel. As in the case of the forwards channel, the transported fluid is most nearly isotonic (for a given set of parameters) when solute input is confined to the closed end of the channel (left-hand side of Fig. 4), and it becomes more hypertonic as the transport mechanism is spread out over increasing fractions of the channel length towards the open end. The explanation is that lower fractions of the channel length are available for osmotic equilibration when solute pumps are nearer the open end. The actual extent of the hypertonicity depends upon the values of other parameters. For instance, with the set of parameters used in the lowest curve of Fig. 4, the transported fluid is still only 9% hypertonic with solute pumps uniformly distributed over the channel length, but it is 23%

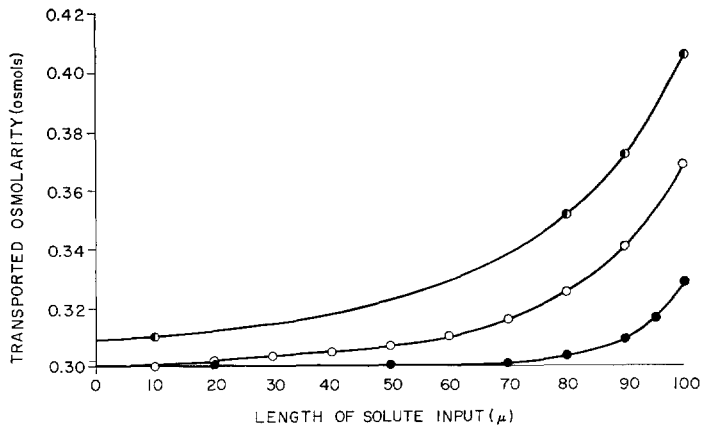

FIGURE 4 The effect of varying solute transport site upon the osmolarity of the fluid transported by a backwards standing-gradient flow system (given by expression 1). L was held at 100 μ, r at 0.05 μ, C_o at 0.3 osmol, and D at 10^{-5} cm^2/sec. P was held at 1×10^{-5} (◐), 2×10^{-5} (○), or 1×10^{-4} (●) cm/sec, osmol. A given solute transport rate (N) held over a range of x from zero out to the value given on the abscissa, and N was zero for x greater than this value. The transport rate for the whole channel was held fixed at $-(2\pi rL)$ (10^{-7}) milliosmols/sec, by choosing N (transport rate per unit wall area, in milliosmols/cm^2, sec) as $-(100)$ (10^{-7}) divided by the length of solute input in microns.

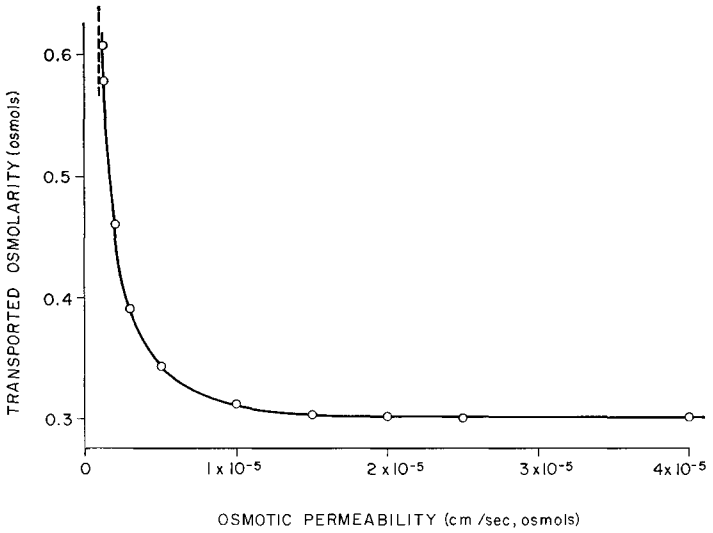

FIGURE 5 The effect of varying channel water permeability (abscissa) upon the osmolarity of fluid transported by a backwards standing-gradient flow system. L was held fixed at 100 μ, r at 0.05 μ, C_o at 0.3 osmol, and D at 10^{-5} cm^2/sec. N was -10^{-6} milliosmols/cm^2, sec for $0 < x < 10\ \mu$ and zero for $x > 10\ \mu$. The dashed vertical lines indicate the minimum possible value of P for this set of values of the other parameters, as limited by the problem of solute exhaustion (see text).

hypertonic under these conditions if channel water permeability is five times lower (middle curve).

Channel Water Permeability (P)

As illustrated in Fig. 5, the transported fluid is hypertonic for low values of P and approaches isotonicity asymptotically for increasing values of P, other parameters being held constant. The same conclusion follows from Figs. 4 and 6. The reason is that the rate of water outflow across the channel walls down the osmotic gradient created by active solute transport varies as the water permeability of the channel walls, so that a closer approach to osmotic equilibrium is achieved in more permeable channels.

Two additional features of Fig. 5 are of interest. One feature is that, as mentioned previously, the problem of solute exhaustion imposes a specific lower limit on possible values of P for a given set of values of the other parameters. With the set used for Fig. 5, this limit is $P = 1 \times 10^{-6}$ cm/sec, osmol and is indicated by the dotted vertical lines in the figure. The other feature is that the relation between P and the transported osmolarity can become quite steep (left-hand side of Fig. 5); this suggests a mechanism by which a hormone modifying the permeability of an epithelium can finely regulate the osmolarity of the transported fluid.

Solute Transport Rate

Fig. 6 illustrates the effect of variations in solute transport rate on the transported osmolarity at three different values of the water permeability (P), other parameters of the system being held constant. At each value of P there is a maximum value of the transport rate N physically possible (indicated by vertical dashed lines), as discussed previously. Below this maximum value the transported osmolarity initially increases slightly with transport rate (N) and then remains constant as N is decreased indefinitely. The transported osmolarity in this rate-independent plateau is a characteristic of each standing-gradient system and depends upon the values of L, r, P, and D. For instance, Fig. 6 shows that the plateau osmolarity becomes increasingly hypertonic for decreasing values of the water permeability P: the plateau is 0.303 osmol for $P = 2 \times 10^{-5}$ cm/sec, osmol, 0.506 osmol for $P = 2 \times 10^{-6}$, and 0.754 for $P = 1 \times 10^{-6}$. As mentioned in the Discussion, these facts may be of physiological significance. Fig. 6 also shows that the maximum sustainable transport rate decreases with decreasing values of P.

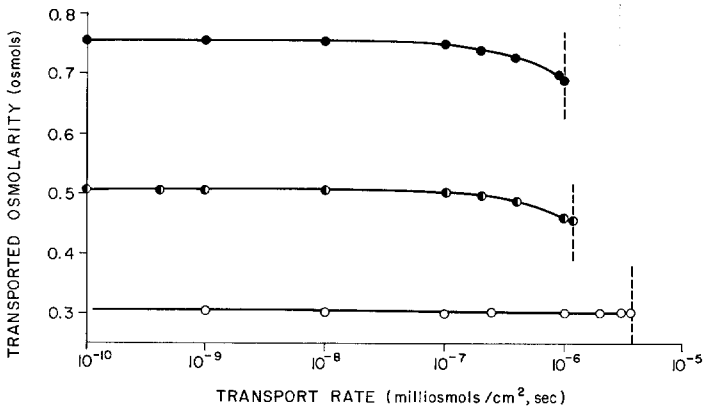

FIGURE 6 The effect of varying solute transport rate upon the osmolarity of fluid transported by a backwards standing-gradient flow system. L was held fixed at 100μ, r at 0.05 μ, C_o at 0.3 osmol, and D at 10^{-5} cm^2/sec. P was 10^{-6} (●), 2×10^{-6} (◐), or 2×10^{-5} (○) cm/sec, osmol. The transport rate plotted on a logarithmic scale on the abscissa holds in the range $0 < x < 10$ μ, and the rate is zero for $x > 10$ μ. The vertical dashed lines indicate the maximum possible transport rate at each value of P, as limited by the problem of solute exhaustion (see text).

Effects of Channel Length and Channel Radius

The transported osmolarity becomes more nearly isotonic, and less hypertonic, as channel length (L) increases or as channel radius (r) decreases. Graphs of transported osmolarity versus L or r are not presented because they are similar to those for the case of the forwards channel (see Figs. 5 and 6 in reference 2). The reason for the closer approach to osmotic equilibrium with increasing L is the greater length over which osmotic equilibration of actively transported solute can take place. The reason for the radius effect is that in narrower channels a given amount of solute will be removed from a smaller volume, creating a larger concentration change, greater osmotic outflow of water, and hence a closer approach to osmotic equilibrium.

DISCUSSION

Most comments about forwards operation of standing-gradient systems and the limitations of this simplified model, which were discussed in detail previously (2), apply equally well to backwards operation and need not be repeated here. For instance, it is obvious that the epithelial structures postulated to function as standing-gradient systems, such as basal infoldings, differ appreciably in shape from right-circular cylinders; but the differential equations which apply to some other simple and sometimes more appropriate geometrical idealizations (e.g. thin cylindrical rings and infinite parallel planes) are identical; and deviations from these idealized geometries are not expected to affect the qualitative conclusions, if the basic principles of progressive osmotic equilibration along long narrow channels are correct. The remainder of this discussion is therefore limited to a few of the distinctive properties of backwards channels, particularly those that differ from the properties of forwards channels, and some resulting predictions.

The basic conclusion is that standing-gradient flow systems can transport fluid in either direction, depending only upon the orientation of the active solute transport mechanism. It therefore comes as no surprise to find secretory epithelia, such as the choroid plexus and Malpighian tubule, that are ultrastructurally very similar to absorptive epithelia, such as renal tubular epithelium. If one took the choroid plexus as a specific example, standing gradients in the basal infoldings might be responsible for water transport from blood to cell; and, more speculatively, gradients in microvilli might be responsible for transport from cell to ventricle lumen. The calculated osmolarities (isotonic up to a few times isotonic) associated with parameter values in the physiological ranges fall in the range of osmolarities actually observed in the choroid plexus, Malpighian tubule, avian salt gland, and rectal gland; this suggests that water

transport in backwards epithelia may follow quantitatively as a geometrical consequence of epithelial ultrastructure. The distinctive plateau-type relation between osmolarity and transport rate illustrated in Fig. 6 duplicates a puzzling physiological property of the avian salt gland, which produces a hypertonic fluid of virtually the same osmolarity at any rate of secretion (11). This property, too, may be a geometrical consequence of the morphology.

Backwards systems differ from forwards systems in three respects. The first difference is the upper limit on the transport rate in backwards systems for a given set of values of the other parameters, as discussed previously. The second difference is that, for transport rates greater than values which give the plateau osmolarity, the transported osmolarity decreases in backwards systems (Fig. 6) but increases in forwards systems (see Fig. 8 in reference 2) with increasing N. At present we have no reason to attribute physiological significance to this difference, and perhaps epithelia will generally prove to be operating with transport rates confined to the plateau region. The third difference is that in backwards epithelia the fluid stream entering the open mouth of the channel will carry not only the solute subject to active transport but also any other solute present in the bathing solution or plasma. Standing gradients of nontransported solutes would consequently be established, with a maximal concentration at the closed end of the channel, depending upon the linear flow velocity, channel length, and solute diffusion coefficient. In backwards epithelia transporting the principal constituent of plasma, NaCl, the effect would involve the minor constituents of plasma and be quantitatively negligible. However, in backwards epithelia transporting a trace constituent of plasma, the effect would operate on the major solutes and could significantly reduce water flow in some circumstances (high velocities, long channels, low diffusion coefficients). This effect does not exist in forwards epithelia where the fluid stream is outwards at the open end. The effect may be the reason why instances of backward channels arise mainly in secretory epithelia, such as the choroid plexus, salt glands of birds and turtles, and rectal gland, whose main secreted solute is NaCl, while secretory epithelia whose main secretory product is a trace constituent of plasma have forwards channels (e.g., intracellular canaliculi in the parietal cells of the stomach, which secrete HCl, and bile canaliculi in the hepatic cells of the liver, which secrete bile salts).

Finally, several predictions can be offered if the basic notion presented in this paper is correct. (*a*) The fluid in basal infoldings, or lateral intercellular spaces, will be hypertonic to the intracellular fluid in forwards epithelia but hypotonic to the intracellular fluid in backwards epithelia. Testing of this prediction will require procedures for solute localization in quick-frozen tissue to prevent dissipation of the gradients. (*b*) Backwards epithelia may prove to have more channels, higher water permeabilities, or lower transport rates than forwards epithelia if they are operating close to the limit of solute exhaustion described earlier. (*c*) It will be interesting to examine whether the apparent correlation mentioned in the previous paragraph, that epithelia secreting the major blood solutes can have either backwards or forwards channels while those secreting solutes present in blood in traces have forwards channels, applies to other cases.

We are indebted to Dr. John McD. Tormey for comments on the manuscript.

Received for publication 10 November 1967, and in revised form 29 January 1968.

REFERENCES

1. Bulger, R. E. 1963. Fine structure of the rectal (salt-secreting) gland of the spiny dogfish, *Squalus acanthias*. *Anat. Record.* **147**:95.
2. Diamond, J. M., and W. H. Bossert. 1967. Standing-gradient osmotic flow: a mechanism for coupling of water and solute transport in epithelia. *J. Gen. Physiol.* **50**:2061.
3. Diamond, J. M., and J. McD. Tormey. 1966. Role of long extracellular channels in fluid transport across epithelia. *Nature.* **210**:817.
4. Diamond, J. M., and J. McD. Tormey. 1966. Studies on the structural basis of water transport across epithelial membranes. *Federation Proc.* **25**:1458.
5. Ellis, R. A., and J. N. Abel, Jr. 1964. Intercellular channels in the salt-secreting glands of marine turtles. *Science.* **144**:1340.
6. Kaye, G. I., H. O. Wheeler, R. T. Whitlock, and N. Lane. 1966. Fluid transport in the rabbit gall bladder. *J. Cell Biol.* **30**:237.

7. KOMNICK, H. 1965. Funktionelle Morphologie von Salzdrüsenzellen. *In* Sekretion und Exkretion. Springer-Verlag, Berlin.
8. PHILPOTT, C. W. 1966. The use of horseradish peroxidase to demonstrate functional continuity between the plasmalemma and the unique tubular system of the chloride cell. *J. Cell Biol.* **31**:86A.
9. PHILPOTT, C. W., and D. E. COPELAND. 1963. Fine structure of chloride cells from three species of *Fundulus*. *J. Cell Biol.* **18**:389.
10. PONTENAGEL, M. 1962. Elektronenmikroskopische Untersuchungen am Ependym der Plexus choriodei bei *Rana esculenta* und *Rana fusca* (Roesel). *Z. Zellforsch. Mikroskop. Anat.* **68**:371.
11. SCHMIDT-NIELSEN, K. 1960. The salt-secreting gland of marine birds. *Circulation.* **21**:955.
12. SCHMIDT-NIELSEN, K., and R. FANGE. 1958. Salt glands in marine reptiles. *Nature.* **182**:783.
13. TORMEY, J. MCD., and J. M. DIAMOND. 1967. The ultrastructural route of fluid transport in rabbit gall bladder. *J. Gen. Physiol.* **50**:2031.
14. WESSING, A. 1965. Die Funktion der Malpighischen Gefässe. *In* Sekretion und Exkretion. Springer-Verlag, Berlin.